




### AUTHOR QUERY FORM

 ELSEVIER	<b>Book: Friedrich-1611165</b> <b>Chapter: CH0027</b>	<b>Please e-mail your responses and any corrections to:</b> <b>E-mail: <a href="mailto:P.Wilkinson@Elsevier.com">P.Wilkinson@Elsevier.com</a></b>
---	--	--

Dear Author,

Any queries or remarks that have arisen during the processing of your manuscript are listed below and are highlighted by flags in the proof. (AU indicates author queries; ED indicates editor queries; and TS/TY indicates typesetter queries.) Please check your proof carefully and answer all AU queries. Mark all corrections and query answers at the appropriate place in the proof using on-screen annotation in the PDF file. For a written tutorial on how to annotate PDFs, click [http://www.elsevier.com/\\_data/assets/pdf\\_file/0016/203560/Annotating-PDFs-Adobe-Reader-9-X-or-XI.pdf](http://www.elsevier.com/_data/assets/pdf_file/0016/203560/Annotating-PDFs-Adobe-Reader-9-X-or-XI.pdf). A video tutorial is also available at <http://www.screencast.com/t/9OIDFhigE9a>. Alternatively, you may compile them in a separate list and tick off below to indicate that you have answered the query.

**Please return your input as instructed by the project manager.**

<b>Uncited references: References that occur in the reference list but are not cited in the text. Please position each reference in the text or delete it from the reference list.</b>		
<b>Missing references: References listed below were noted in the text but are missing from the reference list. Please make the reference list complete or remove the references from the text.</b>		
Location in Chapter	Query / remark	
AU:1, page 838	Please update this reference with page range.	
AU:2, page 821	Please check and confirm the shortened running head.	
AU:3, page 828	Supplied figures 27.6 and 27.10 are of low quality. Please check and provide better quality figures.	



# 27

## Recent advances in shape memory epoxy resins and composites

J. Karger-Kocsis<sup>1,2</sup> and S. Kéki<sup>3</sup>

<sup>1</sup>Department of Polymer Engineering, Faculty of Mechanical Engineering, Budapest University of Technology and Economics, Budapest, Hungary, <sup>2</sup>MTA–BME Research Group for Composite Science and Technology, Budapest, Hungary, <sup>3</sup>Department of Applied Chemistry, University of Debrecen, Debrecen, Hungary

### 27.1 INTRODUCTION

Shape memory polymers (SMPs) and related composites are of emerging smart materials in different applications, especially in biomedical, aerospace, and construction engineering fields. SMPs may adopt one (dual-shape), two (triple-shape), or several (multi-shape) stable temporary shapes and recover their original or permanent ones in dual shape or the previous temporary ones in multi-shape versions upon the action of an external stimulus. The external stimulus may be temperature (set by direct or indirect ways), pH, water, light irradiation, redox condition, etc. In most cases, however, the SMPs are thermosensitive (termed also thermoresponsive or thermally activated) ones. The “switching” or transformation temperature ( $T_{\text{trans}}$ ), enabling the material to return to its permanent shape, is linked with the glass transition ( $T_g$ ) or the melting temperature ( $T_m$ ) [1–3]. Therefore the SMPs are often subdivided based on their switch types into  $T_g$ - or  $T_m$ -based SMPs. As reversible “switches,” however, other mechanisms such as liquid crystallization/melting, supermolecular assembly/disassembly, irradiation-induced reversible network formation, formation and disruption of a percolation network may serve [1–2]. The permanent shape is guaranteed by physical (entanglement, interpenetrating networks) or chemical network (composed of permanent or temporary covalent bonds) structures. The corresponding sites are also termed net points. The temporary shape is set by mechanical deformation above  $T_{\text{trans}}$  and it is fixed by cooling below  $T_{\text{trans}}$  whereby maintaining the mechanical load. However, the deformation temperature may be below  $T_g$  or  $T_m$  of the corresponding polymer, as well.

This is the right place to underline SMPs which are at the same time multifunctional materials since they may integrate multiple structural (high stiffness, strength,

820

Multi-Functionality of Polymer Composites. ISBN: 978-0-323-26434-1  
DOI: <http://dx.doi.org/10.1016/B978-0-323-26434-1.00027-1>  
© 2015 Elsevier Inc. All rights reserved.

toughness) and structural (e.g., load bearing)/nonstructural (e.g., sensing, actuation, self-healing, recyclability, biodegradability) functions [4]. The classification for multifunctionality also holds when the presence of properties, which are not linked with each other, is considered as criterion [5].

p0020 For thermosets, the transformation temperature is the  $T_g$ . During setting the temporary shape, the segments between the cross-links adapt to the external load via conformational rearrangements. The strain energy, stored by this way, is released when the material is unloaded and heated above its  $T_g$  via which the permanent shape is restored. All what is disclosed above is related to one-way (1W) SMPs. This means that the external stimulus activates only the change from the temporary to the permanent shape (dual-shape) or from one temporary to the other one (multi-shape version). Apart from 1W, also 2W SMP systems, featuring a reversible shape change on the basis of “on–off” switching of the external stimulus, exist.

p0025 The shape memory (SM) properties are typically quantified by the shape fixity ( $R_f$ ) and shape recovery ratios ( $R_r$ ).  $R_f$  means the extent of fixing of the externally applied deformation in the temporary shape. Its value is 100% when the applied deformation, introduced above  $T_{trans}$ , is fully kept below  $T_{trans}$  in the temporary shape. The deformation modes cover tension, compression, bending, and torsion.  $R_r$  is the percentage of the recovery of the original shape when the material heated above  $T_{trans}$  subsequently.  $R_r = 100\%$  when the original shape of the material is fully restored.  $R_f$  is more frequently used to describe the SM performance. SM properties are often determined in cyclic (one or more) thermomechanical tests performed under stress- or strain-controlled conditions. Figure 27.1 displays the course of an SM thermomechanical test. Beside  $R_f$  and  $R_r$ , further SM characteristics, such as the temperature interval of recovery, recovery rate and recovery force, can be measured.

s0015

## 27.2 SHAPE MEMORY EPOXY (SMEP) FORMULATIONS

p0030

Preferred thermoset SMPs are epoxy (EP) resins based ones. EPs are selected owing to their favorable properties (heat and chemical resistance, high stiffness in both glassy and rubbery stages, good adhesion to many substrates) and versatility (easy tuning of  $T_g$  and of the glassy and rubbery moduli). Next we shall give an overview on shape memory epoxy(SMEP)-based systems and composites. Our intention was to introduce the basic strategies on how to tailor the network structure and performance of SMEPs in order to meet the requirements of given applications. Note that a large body of works was already dealing with various aspects of SMPs [1–3,5–8], and even SMEP was topic of review [8].

s0020

### 27.2.1 NEAT EPs

p0035

As mentioned before, the chemistry of EP resins is flexible enough to tailor the  $T_g$  and thus also the  $T_{trans}$  upon request. The basic formulation tools differ whether the EP/hardener ratio is stoichiometric or not. Off-stoichiometry itself results in

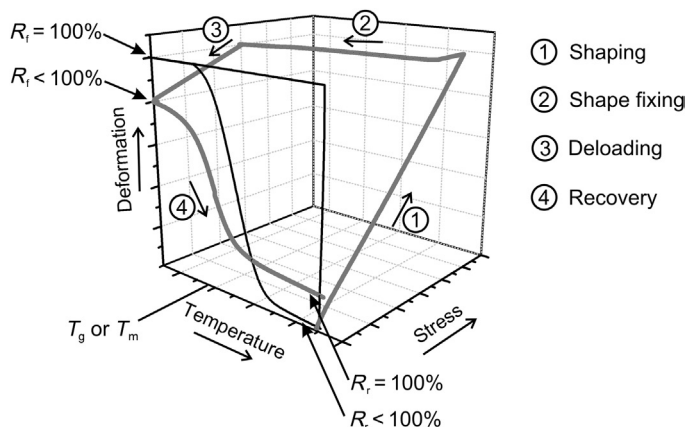


FIGURE 27.1

Single SM cycles of a 1W-SM polymer (black) and its composite (grey), schematically. *Note:* The related traces highlight differences in the mechanical loads, needed for shaping the polymer and its composite, and in the SM characteristics ( $R_f$  and  $R_r$ ).

reduced  $T_g$  values. It is practiced usually by adding less hardener than required by the stoichiometric ratio rather to adding more. For example,  $T_g$  values between 45°C and 145°C can be measured for a bisphenol A-based bifunctional EP cured with aromatic diamine when the curing degree is varied between 50% and 100% (corresponding to the stoichiometry) [9]. This change is accompanied with an almost threefold increase in the cross-linking density. Researchers, however, prefer to use fully cured EPs, formulated by stoichiometric amount of hardener. Even in the latter case, there are numerous possibilities to manipulate the buildup of the network along with the related properties. Strategies for network architecturing target changes from both resin and hardener sides. For amine-cured EPs for example the following options may be selected: combined use of mono- and difunctional amines [10–12], same type of diamines but with various chains length and thus with various amine equivalent weights [11–12], common use of aliphatic and aromatic EPs [11,13] and their variations. Similar versatility exists also for anhydride cured EPs [14]. Figure 27.2 demonstrates how efficiently both EP and hardener types may be used to tune the basic viscoelastic properties ( $T_g$ , glassy and rubbery modulus:  $E_g$  and  $E_r$ , respectively) of a given EP resin.

Rousseau [15] pinpointed that the excellent  $R_f$  and  $R_r$  values ( $\geq 95\%$ ) for SMEPs are due to their high  $E_g$  and beneficial network-given rubber elasticity above  $T_g$ . Like all polymers, also SMEPs are viscoelastic materials. This means that the properties depend on both temperature and time. In the time scale especially heating/cooling and physical aging [16], effects should be taken into consideration. Viscoelasticity implies a strong influence of the selection of  $T_{trans}$  on the SM properties.  $T_{trans}$  is traditionally higher than  $T_g$  (by  $\geq 15\text{--}20^\circ\text{C}$ ).  $T_{trans}$  may be, however, at the vicinity

f0010

p0040

## 27.2 Shape Memory Epoxy (SMEP) Formulations 823

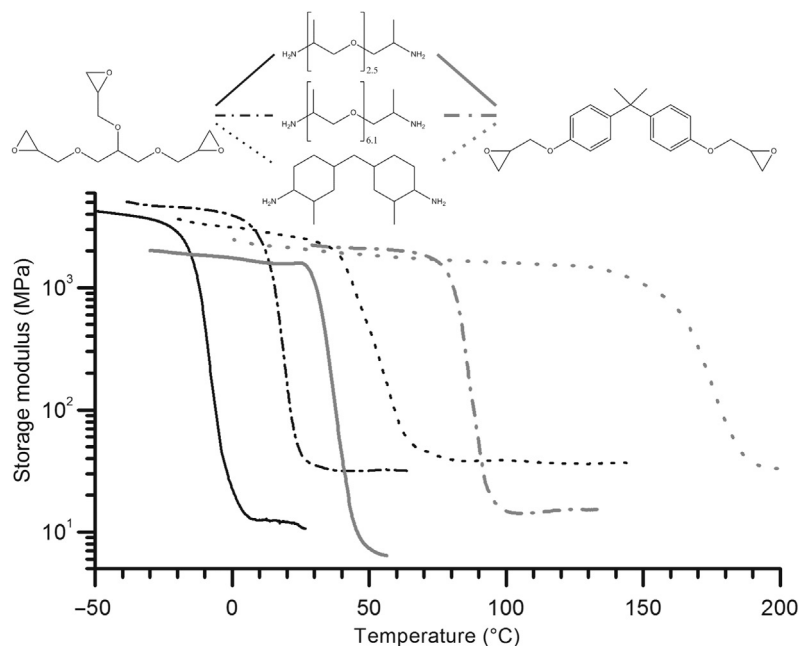


**FIGURE 27.2**

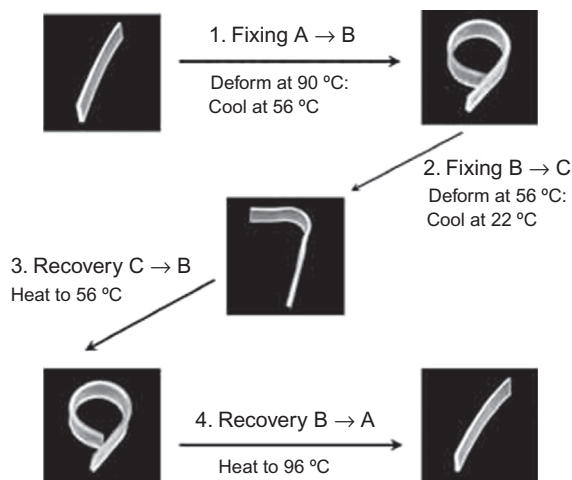
Effects of selected formulations (types of resin and hardener) on the viscoelastic response of amine-cured EPs.

or even below that of  $T_g$ . It is known that the network deformability goes through a maximum when passing  $T_g$  from the glassy to the rubbery state. Feldkamp and Rousseau [17] showed a fivefold increase in the stress–strain response for an EP when it was deformed at the onset of  $T_g$  instead of above  $T_g$ . The thermomechanical recovery process highly depends whether  $T_{trans}$  was above or below  $T_g$  of the corresponding EP. Liu et al. [18] demonstrated in a detailed study that the stress–strain response of shaping above  $T_g$  agrees well with that of the recovery, occurring always above  $T_g$ . By contrast, when shaping was done below  $T_g$ , the recovering stress–strain response differed markedly from the one measured at the shaping temperature. In the latter case, the recovery stress upon flexure peaked at  $T_g$  with a maximum value much smaller than measured upon shaping at  $T_{trans}$ . Moreover, with increasing cooling rate during shape fixing the temperature needed to reach  $R_f = 100\%$  was shifted toward lower temperatures. This was associated with an increasing level of the recovery stress. Understanding the coupling between cooling (shape fixing) and heating rates (shape recovery) and the evolution of the recovery response is a key issue for many applications. This aspect was addressed in a recent in-depth study by Pandini et al. [19]. The cited authors studied the effects of network architecture of the SM behavior of SMEPs under both dynamic and isothermal recovery conditions.

Temporary shaping of the resins was done at  $T_{\text{trans}} < T_g$ , termed to as “cold working.” This kind of thermomechanical programming was argued to be less time-consuming, easier to perform, and bringing additional benefits (improved stress–strain behavior) than the traditional one at  $T_{\text{trans}} > T_g$ . It was found that  $R_f$  decreased with increasing difference between  $T_g$  and  $T_{\text{trans}}$  (i.e.,  $T_g - T_{\text{trans}}$ ). It is noteworthy that the  $R_f$  data for the “cold worked” EPs were somewhat below those of the traditionally deformed (i.e.,  $T_{\text{trans}} > T_g$ ) counterparts. A further important conclusion of Pandini et al. [19] was that the SM recovery behavior is governed by the cross-linking density and the stiffness of the segments in between the net points plays a minor role.

p0045

There are two possibilities to produce multi-shape SMEPs using neat EP resins: (i) exploitation of the “width” of the  $T_g$  range and (ii) preparation of layered systems composed of two or more EPs with different  $T_g$ s. The former approach assumes that the  $T_g$  range can be split into several sections in which a fraction of the segments is in the rubbery while the others in the glassy state. Basic prerequisite of multi-shaping is that the energy stored by deformation of the rubbery segments should be sufficient enough for shape fixing upon cooling and thus guaranteeing the recovery. According to the authors knowledge, this has not yet proven for SMEPs. The feasibility of the “layering” strategy has been demonstrated by Xie et al. [20]. They produced EP bilayers exhibiting triple-SM performance (Figure 27.3). The bilayer system consisted of two EPs with different  $T_g$  values which were hold together by cocuring. The modulus–temperature trace of the bilayers showed two distinct  $T_g$ s followed by two well-developed rubbery plateaus. The two  $T_{\text{trans}}$  values, required for triple-shape performance, were selected from each rubbery plateau section. For the two temporary



f0020

FIGURE 27.3

Triple-SM effect realized with a bilayer composed of two EPs with different  $T_g$ s (lying at about 40°C and 80°C, respectively).

([20], reproduced with permission of Wiley-VCH).



## 27.2 Shape Memory Epoxy (SMEP) Formulations 825

shapes, the  $R_f$  values scattered between 71% and 97% whereas the corresponding  $R_r$  values between 92% and 99%. These ranges depended on the relative thickness ratio of the bilayer constituents.

p0050

Wang et al. [21] argued that by exploiting the  $T_g$  difference even a 2W SMEP system can be created. The proposed system consists of a film surrounding a conical core whereby the  $T_g$  of the latter ( $T_{g2}$ ) is lower than that of the film ( $T_{g1}$ ). Like the bilayer, the composite cylinder is also cocured and thus there is an efficient stress transfer between the covering film and core. Shaping occurs above  $T_{g1}$  and fixing under load by cooling below  $T_{g2}$ . Heating the cylinder to a temperature between  $T_{g2}$  and  $T_{g1}$  its core tends to recover the original shape. The related radial contraction causes microbuckling in the cover film. So, the smooth cylinder transforms into a gear-like shape. Further temperature increase above  $T_{g1}$  yields the complete recovery of the original shape. However, this concept only meets the requirement of a triple-shape system (high temperature temporary shape: smooth compressed cylinder, low temperature temporary shape: partly compressed cylinder with folded surface) and thus erroneously termed to 2W version.

s0025

### 27.2.2 EP RUBBER

p0055

EPs are brittle materials due to their tightly cross-linked network. Their toughening has become a topic of research which is still ongoing. One of the early toughening strategies was to generate particles which are micron- or nanoscaled dispersed in the EP. These particles cavitate and participate in crack pinning. Moreover, they facilitate the shear deformation of the EP ligaments between the particles which is the major energy absorbing mechanism [22]. The in situ generated particles are from functionalized or nonfunctionalized rubbers, which are initially dissolved in the curable EP but segregate during the gelling/cross-linking of EP. For EPs the most powerful toughening agents are end-functionalized liquid nitrile rubbers though their use is accompanied with penalties especially in water uptake, stiffness, and  $T_g$ . Amine- and carboxyl-terminated acrylonitrile-butadiene rubbers (ATBN and CTBN, respectively) are preferred tougheners of EP. Note that their incorporation loosens and distorts the network depending on the reactive or nonreactive nature of the modifiers. This, accompanied with increased ductility, should affect the SM behavior of the corresponding EPs that has been already investigated. CTBN incorporation did not influence  $R_f$  and  $R_r$  (both remained close to 100%) but markedly increased the number of thermomechanical cycles that could suffer the related system without failure [23,24]. Modification of EP with carboxyl-terminated polyurethane (PU) yielded reduced  $T_g$  and enhanced ductility, similar to CTBN. The related blend exhibited excellent SM performance in fold-deploy tests [25].

s0030

### 27.2.3 EP THERMOPLASTIC

p0060

To avoid the disadvantages with rubber tougheners, many works were dedicated to the toughening of EPs with amorphous or semicrystalline thermoplastics. Though their toughening mechanisms are essentially the same as for rubber modifiers, their





826 CHAPTER 27 Recent advances in SMPs and composites

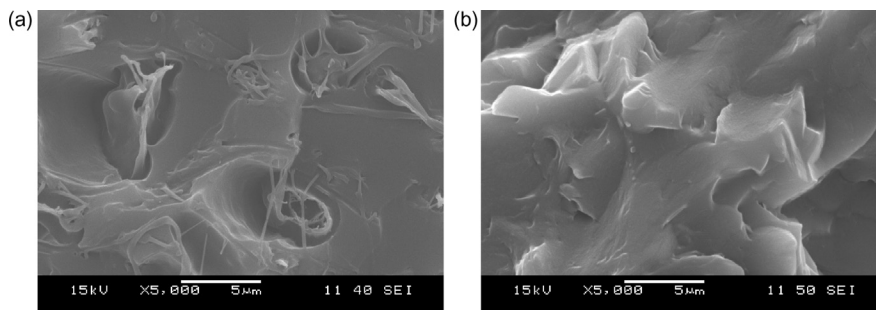
incorporation is not associated with pronounced reductions in the basic mechanical and thermal properties. Great variety of thermoplastic polymers has been tried to modify EPs, such as polymethyl methacrylate, linear (co)polyesters, polyethylene oxide, poly( $\epsilon$ -caprolactone) (PCL), polyoxymethylene, polyamide, styrene copolymers, polyphenylene oxide, and various high temperature resistant thermoplastics (mostly amorphous ones) [26]. Interestingly, thermoplastic modified EPs were not yet subjected to SM testing. Nonetheless, researchers made use of the related knowledge. To demonstrate this fact, SM performance of EP/PCL combinations will be introduced next. Note that PCL is a semicrystalline biodegradable polyester having a  $T_m$  of about 60°C which is highly preferred as blend component and network constituent in various biodegradable SMPs [27].

p0065 Lützen et al. [28] produced a conetwork containing cationically polymerized EP covalently linked with hydroxyl-terminated semicrystalline PCL. Chemical reaction occurred between the hydroxyl groups of PCL and EP groups of the EP resin. The PCL content was varied between 60 and 85 wt%. It has to be born in mind that  $T_{trans}$  was linked with  $T_m$  of PCL in this conetworked EP/PCL system. The usually quoted benefit for  $T_m$ -based SMPs is that the shape fixing is better and the recovery is faster than in  $T_g$ -based ones.  $R_f$  was 100% and changed marginally with the PCL content in fold-deploy tests opposed to  $R_r$  that decreased with increasing PCL content.

p0070 Luo and Mather [29] found an elegant way to produce triple-shape memory EP system. Opposed to the bilayer principle [20], they followed another strategy: electrospun PCL was embedded in an EP matrix.  $T_g$  of the EP, set by combination of aliphatic and aromatic versions, was below the  $T_m$  of PCL. Temperature of the EP curing occurred below  $T_m$  of PCL. Through infiltration of the PCL nanoweb by EP, a system of bicontinuous structure was formed. For programming of the two temporary shapes, set by different tensile deformations (second shaping at higher deformation than at the first one),  $T_m$  of PCL and  $T_g$  of EP were considered thereby choosing  $T_{trans,high} = 80^\circ\text{C}$  and  $T_{trans,low} = 40^\circ\text{C}$ , respectively. The EP/PCL system was tested for both dual and triple-SM performances. In the former case, both  $R_f$  and  $R_r$  were close to 100%. During triple-shape tests the  $R_f$  and  $R_r$  data, measured for the second shape, were lower than for the first one. A similar approach was followed by Fejős et al. [30]. These authors incorporated also graphene into the PCL containing solution to be electrospun. This was aimed at facilitating the infiltration by EP via reinforcing the nanoweb. A new aspect in this study was to check whether the creation of a thermodynamically induced cocontinuous morphology results in SM properties comparable with the EP/electrospun PCL nanoweb system. The cocontinuous structure in this case is a semiinterpenetrating (semi-IPN) one because one of the continuous phases is thermoplastic (PCL) while the other is thermoset (EP). This semi-IPN was achieved by dissolving the PCL, the amount of which agreed with of the nanoweb in the reference system, in the EP followed by curing of the latter. EP/PCL with bicontinuous phase and semi-IPN structures are shown in Figure 27.4.

p0075 The storage modulus–temperature curves are similar for the EP/PCL systems irrespective to their structures (Figure 27.5). The difference can be ascribed to preparation-related effects.

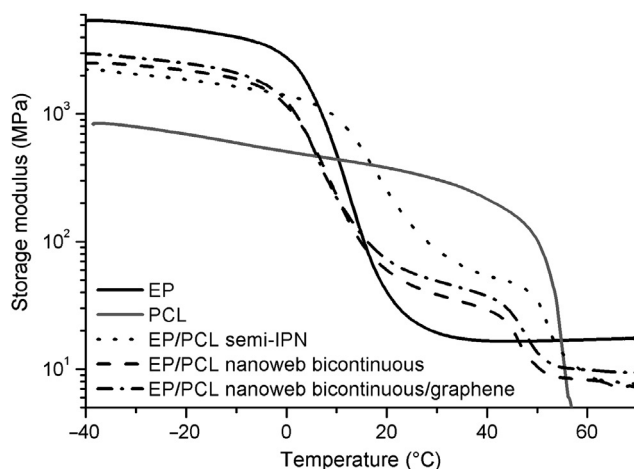




f0025

FIGURE 27.4

Scanning electron microscopic (SEM) pictures taken from the EP/PCL with (a) bicontinuous (via embedding a PCL nanoweb) and (b) semi-IPN structures.



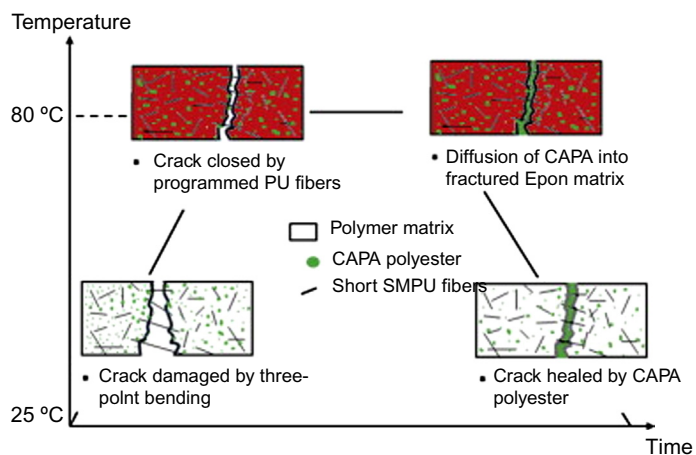
f0030

FIGURE 27.5

Storage modulus as a function of temperature for the EP/PCL with different structures and their plain constituents. *Note:* PCL content is 23 wt%.

p0080

Triple-SM tests were performed in a dynamic mechanical analyzer at two different tensile strains thereby increasing the strain from the first to the second shaping. It was found that graphene incorporation into the PCL nanoweb negatively affected the  $R_f$  and  $R_r$ . Graphene was incorporated into the PCL containing solution to be electrospun in order to improve the properties of the resulting PCL nanofibers. On the other hand, the  $R_f$  and  $R_r$  for both temporary shapes of the EP/PCL with semi-IPN structure were comparable with those of the EP/PCL nanoweb. Moreover, the semi-IPN structured EP/PCL outperformed the EP/PCL nanoweb with respect to  $R_f$  linked with the



AU:3

f0035

**FIGURE 27.6**

Schematic of the two-step healing process (i.e., close-then-heal) in a fractured short SMPU fiber-reinforced specimen.

([32], reproduced with permission of Elsevier).

first temporary shape. Based on this result, a bright future can be prophesied for the development of SMP systems with semi-IPN structure. This quote is supported by another aspect. Semi-IPN structured systems may overtake a further functional role, namely self-healing. This concept, i.e., combination of shape memory and self-healing, has been recommended by Karger-Kocsis as cited in Ref. [31]. In semi-IPNs, the thermoplastic polymer (amorphous or semicrystalline) offers “switching” (SM) and “healing” (molecular entangling) effects, whereas the cross-linked thermoset acts for fixing of the permanent shape.

p0085

It has to be mentioned that incorporation of thermoplastic micro- and nanofibers in various forms (short, mat) into EPs may contribute to shape memory assisted self-healing, as well. For that purpose one has to find suitable polymers, polymer fibers, well adhering to the EP, which exhibit prominent strain hardening. The latter is usually accompanied with crystallization. To support the healing, however, a thermoplastic phase should be present. The feasibility of this concept has been shown using short SM PU fibers embedded in EP containing a dispersed PCL phase (Figure 27.6) [32]. It is obvious that this strategy could be well adapted for semi-IPN EP/PCL systems and even better performance can be prophesied.

s0035

#### 27.2.4 EP THERMOSET

p0090

Albeit many EP systems with full-IPN structure, meaning that both continuous phases are cross-linked, have been synthesized, they were not tested for SM properties. This is very surprising considering the fact that such full-IPN systems have a

broad  $T_g$  range, sometimes even with two peaks due to incompatibility. Recall that the latter are key factors for MPs with multi-shape feature.

p0095

The EP combinations, which fall into the above category, are basically conetworks. Conetworks are chemically cross-linked networks in which none of the constituents forms a continuous phase. This definition does not exclude however the possible presence of domains which are rich in one or in other of the constituents. For the creation of EP containing conetworks with SM properties, the epoxy-isocyanate (oxazolidone formation) and epoxy-isocyanurate (oxazolidinone formation) reactions were used [33,34]. The oxazolidone chemistry is a useful way to tailor the hard segments in PUs [33]. Note that segmented PUs represent the most versatile and mostly researched family of SMPs [35]. The conetwork formation of hybrid resins containing EP, cyanate ester, and phenol-terminated diol is a very complex process owing to the onset of different chemical reactions. Figure 27.7 suggests that these reactions yield a rather inhomogeneous conetwork. This is well manifested in a broad range of the mechanical loss factor ( $\tan \delta$ ), which may even show two peaks. The latter, assigned to polyisocyanurate-rich (high temperature) and polyol-rich segments (low temperature), is a clear appearance of incompatibility.  $R_r$  increased with increasing  $E_g/E_r$  ratio for this hybrid by contrast to the recovery time that showed an adverse trend.

p0100

Interestingly, the benzoxazine chemistry was not yet used though very versatile, especially in combinations with EPs [36–38].

s0040

## 27.3 SHAPE MEMORY EP COMPOSITES

p0105

Research on SMPs was extended for related composites from the early stage. This was fueled mostly by two facts: (i) need for other triggering mechanisms of the shape recovery than direct heating and (ii) great demand for SM polymeric systems featuring fast recovery along with high recovery forces. The latter is essential for actuators, which is favored target application of SMP systems. Next it will be demonstrated that the above properties were achieved by (nano)fillers and traditional reinforcements, respectively.

s0045

### 27.3.1 PARTICULATE-FILLED

p0110

Micro- and nanoparticulates used in polymers may be grouped according to their appearance: spherical (low aspect ratio), disc-like, and fibrous (high aspect ratios). Next we shall report following this grouping. Liu et al. [39] checked the SM properties of EPs containing 20 wt% SiC of 700 nm mean size. Temporary shape was set both above and below that of the  $T_g$  of the related composite. The nanocomposite generated higher recovery stress than the unfilled matrix. It is noteworthy that SiC is a very efficient filler to enhance the thermal conductivity of the corresponding matrix. This is a key issue for thermally activated SMPs. However, direct heating is not always practical, and thus researchers were looking for its alternatives. Indirect

830 CHAPTER 27 Recent advances in SMPs and composites

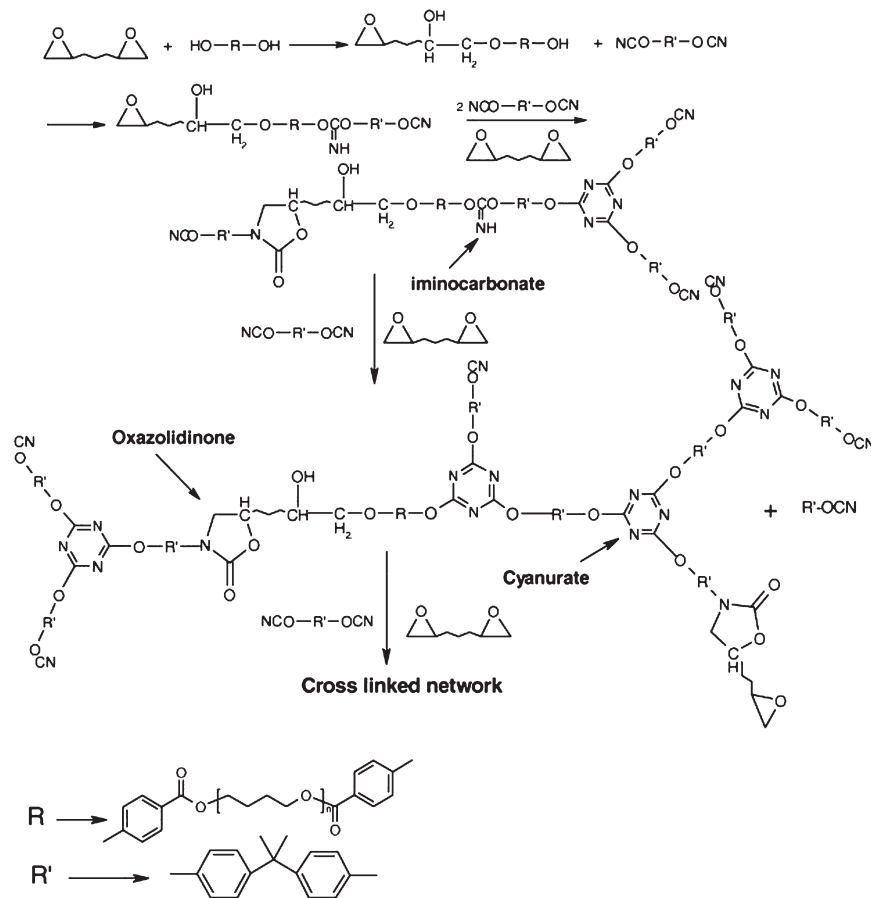


FIGURE 27.7

Possible reaction pathway for conetwork formation in a hybrid systems composed of EP, cyanate ester (–OCN groups) and phenol-terminated polyol.

([34], reproduced with permission of Elsevier).

heating can be achieved for example by adding infrared absorbing, electrical (Joule heating) and magnetic conductive (inductive, hysteretic heating) fillers. Some of them, such as infrared irradiation, absorption of radiofrequency energy, may result in wireless, remote actuation of SMPs. Hazelton et al. [40] showed the feasibility of radiofrequency actuation of EP containing magneto-electroelastic particles, added in  $\leq 15$  vol.%. Surface modification of nanofillers may be also a tool of tuning the SM properties. Iijima et al. [41] modified the surface of  $\text{TiO}_2$  nanoparticles with an anionic surfactant having a polyethylene glycol (PEG) chain, large enough for crystallization.  $T_m$  of PEG of these “PEGylated”  $\text{TiO}_2$  particles could be used as  $T_{\text{trans}}$  when embedded in an EP matrix in  $\leq 13$  wt% amount.

p0115 Organophilic clays of disc-like structure have been incorporated in EP systems in order to improve their (fracture) mechanical performance. Their effect has been checked also with respect to SM. It was found that organoclay in 3 wt% enhanced the recovery speed without reducing  $R_r$  [42]. Beloshenko et al. [43] added thermoexpanded graphite (which belongs to the disc-like fillers, too) with and without kaolin microparticles in EP, and studied the SM properties in uniaxial compression. Though no Joule heating was found, meaning that the material remained insulator, the resistivity of the composites increased steeply at the  $T_g$  of the resin.

p0120 Lu et al. [44] combined electrical conductive carbon nanofiber (CNF) with electromagnetic Ni nanostrands to render the initially insulating EP to electric conductive. The resulting SMEP was activated by electrical resistive heating (Joule effect) and displayed very fast recovery. This was supported also by the high thermal conductivity, being a “byproduct” of the filler combination used. Untreated and silanized vapor-grown CNF was incorporated in EP to improve its SM performance recently [45]. Silane surface treatment served for a better dispersion of CNF in the EP matrix. CNF presence caused a significant change in the  $T_g$  of the EP because the silane contained  $-NH_2$  functional groups, reactive with the EP. The shape recovery of the EP was improved by CNF dosage, and the recovery ratio was further enhanced when silanized CNF replaced the untreated one in the corresponding formulation.

### s0050 27.3.2 FIBER- AND FABRIC-REINFORCED

p0125 As reinforcements in EP-based composites, various fiber assemblies are traditionally used. Their range covers nonwoven mats, different woven structures, and fabrics with unidirectional (UD) fiber alignment. UD fibers are usually present in prepregs from which advanced composite laminates with various lay-ups are produced. Nowadays, UD fiber containing fabrics, even composed of two or more different materials (hybrid reinforcement), are on the market. The reinforcing fibers may be of synthetic (glass, carbon, aramide) or of natural origin (mineral fibers such as basalt, plant fibers such as flax, jute, sisal, and the like). The stiffness and strength of the reinforced EPs are prominently higher than those of the matrix, moreover, they can be tuned upon request by different ways (e.g., type and amount of the reinforcement, fabric layering, and orientation). High stiffness and strength are desirable properties for the recovery of SMEP composites in order to compete in some applications with shape memory alloys (SMAs). Therefore great efforts are undertaken to prepare SM polymeric composites with enhanced recovery stress and reduced recovery time. Unfortunately, reinforcing with fibrous structures, especially when present in high amount in the related composite, reduces the ductility and deformability thereby restricting the design freedom for temporary shaping. So, improved recovery stress is usually achieved at expense of the shaping deformability. In some cases, for example during bending of UD fiber containing laminates, this drawback is circumvented via a peculiar deformation of the fibers. They undergo microbuckling in the compressed zone of the specimen or part thereby realizing relatively high deformations [46–48]. Accordingly, an advanced EP-based composite with high UD carbon fiber (CF)

content may exhibit at about 5% nominal bending strain, though the ultimate strain of the CF is <1% [47]. To make use of this microbuckling, however, attention should be paid on the right selection of the matrix, fiber/matrix adhesion and adjustment of the shape programming procedure to the composite's properties. Basit et al. [49–51] prepared layered composites with symmetric and asymmetric hybrid reinforcements and studied their SM properties in bending mode both in unconstrained and constrained conditions in cyclic tests. Note that unconstrained testing is accompanied with stress free deformation and thus suited to determine  $R_f$ . By contrast, constrained deformation is performed under load based on which the recovery stress can be measured. The cited authors made use of the Joule heating, produced via UD CFs embedded in the mid-section (neutral axis) of the specimens, to set  $T_{\text{trans}}$  for temporary shaping and to get those temperatures where the shape recovery was investigated. This system worked basically as an actuator. The recovery stress developed was studied as a function of  $T_{\text{trans}}$  and recovery temperature.

There are further possibilities to widen the shaping freedom with SMEP composites. It is intuitive that the higher the deformability of a given composite the lower the content of the fabric reinforcement. That is the reason why SMEP composites usually do not contain more than 60 wt% reinforcement. Positioning of the reinforcing layers along with the types of the reinforcements may affect the deformability, as well [52]. Just one example to underline the latter: a fabric with the same pattern and surface weight has completely other deformability when produced from stiff CFs instead of more “compliant” natural fibers (NF). These are the main topics addressed by the actual research with SMEP composites as displayed below.

Four GF fabric layers were infiltrated by EP yielding a composite with rather high reinforcement content (38 vol.%). It was found that with increasing GF fabric content  $R_f$  decreased opposed to the recovery stress that was enhanced by 1 order of magnitude (ca. 40 MPa). Parallel to that the critical bending strain, not causing observable damage, was highly reduced compared to neat EP (from >6% to 1%) [53]. In a follow-up study, Fejős and Karger-Kocsis [54] studied the SM properties of CF fabric-reinforced composites in bending. The CF layers were either on the tensile or on the compression side of the specimens during unconstrained and constrained tests. Again, the critical bending strain for SM testing was highly reduced by the reinforcement. The temperature and stress developments as a function of time are depicted in Figure 27.8 for the EP and EP/CF composites with CF layers positioned on the top (compression side) and bottom (tensile side), respectively. One can notice that the stress values needed for deformation and measured during recovery agree well with each other. This implies good  $R_f$  and  $R_r$  data which were >93%, in fact. For the shape fixing required stress of the specimen containing CF layers on the top (under compression) was, however, much higher than the recovered one. This suggests the onset of microbuckling associated with an increment in the elastically stored energy. A substantial part of this is released, however, before passing the  $T_g$  of the EP matrix—see the courses of apparent stress and temperature in the related time interval in Figure 27.8.

This finding suggests that reinforcing layers of such SM composites which are designed to deliver high recovery stress should stay under compression and their recovery should be triggered at the onset of  $T_g$  or below. Recall that this recommendation

p0130

p0135

p0140



## 27.3 Shape Memory EP Composites 833

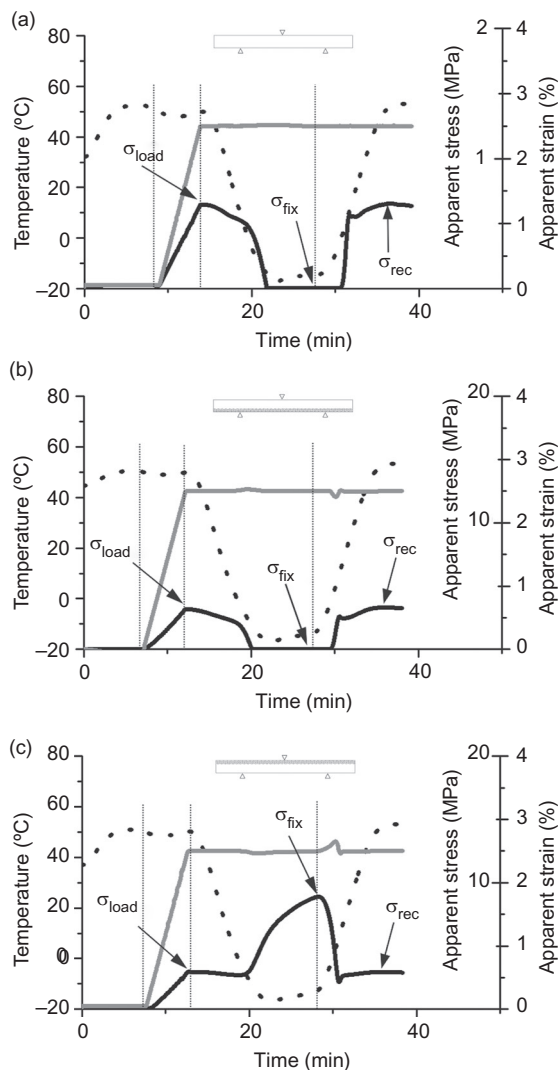


**FIGURE 27.8**

Shaping and recovery cycles of the neat EP and its asymmetrically positioned CF fabric (2 layers) reinforced composites in bending.

(based on Ref. [54]—with permission of BME-PT).

is in full agreement with that of gained from studies on SMEP composites, termed also to as elastic memory composites [46–48]. It has to be underlined that EP reinforcement with just two layers of CF fabric increased the recover stress by 1 order of magnitude compared to that of the matrix (Figure 27.8).



## 834 CHAPTER 27 Recent advances in SMPs and composites

p0145 Following the actual research trend, attempt was made to produce SMEP composites from fully renewable resources. To produce a “biocomposite” epoxidized linseed oil, cured by anhydride, was selected as matrix, and flax fabrics (nonwoven mat, twill-weave, and quasi UD fabric) served for reinforcement [55]. Recall that NF may be a favored reinforcement for SMEP because its presence imparts the deformability of the corresponding composite in lesser extent than traditional reinforcing fibers. The flax fiber content (<58 wt%) was varied through the number of fabric layers, their surface weight and fineness of the flax fibers. The  $R_f$  and  $R_r$  data of this epoxidized linseed oil-based EP were 92% and 25%, respectively. The very low  $R_r$  substantiates that the recovery performance is controlled by the cross-link density, which was much lower in this “bioresin” than in typical “petro-based” EPs.  $R_f$  was reduced and  $R_r$  improved by the flax reinforcement, though they remained still moderately low [55]. This study also revealed that the fabric type and its architecture with respect to the loading direction have a strong impact on the SM properties.

p0150 Albeit there is a vast knowledge on EP-based composites, it is not yet translated for optimizing their SM possibilities. This note holds for all reinforcement-related issues and even for loading mode adapted for temporary shaping (e.g., torsion is disregarded).

s0055

### 27.4 APPLICATIONS

p0155 SMEPs and related composites are gaining in importance in different application fields due to their multifunctionality. SMEP composites are promising candidate materials for various parts of space (e.g., solar arrays, antennas, booms, deployable panels, reflectors) [56–58] and aircrafts (different morphing concepts for wing parts and skins) [59,60]. This is owing to their good SM properties, excellent stiffness, strength, and environmental durability. Note that space structure should be transported in compact forms. The term packaging/deployment in this field is translated for temporary shaping/shape recovery in terms of SMPs. The packaging/deployment, however, should be adjusted to the composites’s properties. This requires the understanding of the failure during “packaging,” i.e., setting and fixing of the temporary shape [60].

p0160 Combination of SMEP and its composites with SMAs may result in multifunctional smart material systems. Multi-state smart bias systems (such as smart valve) with varying stiffnesses can be obtained by varying the  $T_g$  of the SMEP between the related  $T_{trans}$  values of SMA, i.e., martensitic finish and austenitic finish temperatures [61,62]. It is noteworthy that the stiffness during “switching” changes adversely for SMP and SMA (Figure 27.9). Figure 27.9 also highlights the large difference in the stiffness data between SMP and SMA. Hybridization of SMEP with SMA wire is an interesting tool to produce triple-SM composites as shown in Figure 27.10.

p0165 Multilayer SMEP composites may be used for orthopedic casts supporting the healing of bone fractures [63]. Based on the bilayer strategy with SMEPs, the gecko adhesion (attachment/detachment to the surface) can be imitated, as demonstrated by Wang et al. [64].



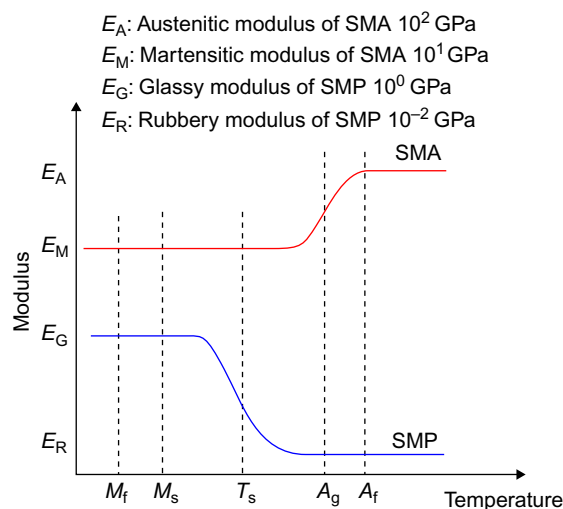


**FIGURE 27.9**

Modulus as a function of temperature for SMP and SMA, schematically. *Note:* This figure emphasizes the effect of the corresponding transformation (“switching”) temperatures.

([62], reproduced with permission from Elsevier).

## 27.5 OUTLOOK AND FUTURE TRENDS

The chemistry of EP curing is well known. Thus we have all the necessary tools to tailor  $T_g$  and thus  $T_{trans}$  upon request for SM performance. Nonetheless, even here we can trace some less explored fields, such as EP-based full IPNs and conetworks, which require further attention and are very promising to tune the SM properties. Recall that conetworks and full IPNs may show multi-shape properties. EP-based semi-IPNs may combine SM and self-healing functionalities as argued before. Components of SMEPs can be selected from renewable resources. Vivid development can be expected for SMEP composites. As reinforcements NF-based fabrics, allowing high deformability, will be progressively used. Benefits of reinforcement hybridizations will also be studied with respect to SM performance. The target with traditional reinforcements is to find their necessary amount and lay-up which yields the highest storage of elastic energy thereby maintaining high deformability for a given loading mode. To support the related research, SM cycling tests will be followed by suitable nondestructive testing techniques. Mapping of the failure mode will help to deduce guidelines for packaging/deploying, i.e., temporary shaping/recovery. Research work will be intensified to replace direct heating by other means for the shaping and recovery. For this purpose, the inherent properties of traditional reinforcements, such as the electric conductivity of CF, will be combined with other desired properties (e.g., thermal conductivity) given by (nano)fillers. The combination of SMEP with SMA remains a hot topic

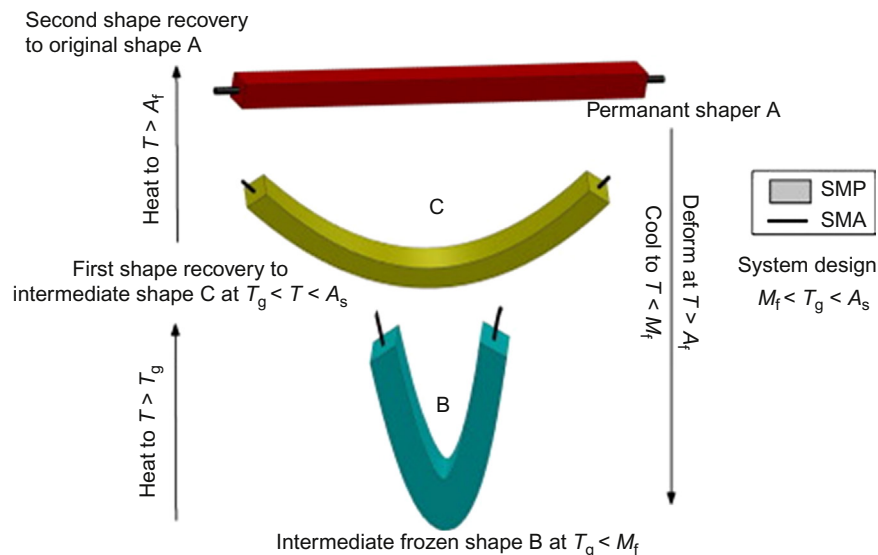


FIGURE 27.10

Three-state configuration (triple-SM) obtained by SMEP and SMA wire. Note: For designations cf. Figure 27.9.

([62], reproduced with permission from Elsevier).

with many challenges (optimum amount of SMA including its structuring, adhesion of SMA to the matrix, modeling the properties [65]). The future belongs to “active” SMEPs and related composites. “Active” means the adaptability of the material to give an adequate response to varying external stimuli.

## ACKNOWLEDGMENTS

The work reported here was supported by the Hungarian Research Fund (OTKA NK 83421) and by the TÁMOP-4.2.2.A-11/1/KONV-2012-0036 project co-financed by the European Union and the European Social Fund. Part of this work was also supported by the European Union and the State of Hungary, co-financed by the European Social Fund, in the framework of TÁMOP-4.2.4.A/2-11/1-2012-0001 “National Excellence Program” (S.K.).

## REFERENCES

- [1] Hu J, Zhu Y, Huang H, Lu J. Recent advances in shape-memory polymers: structure, mechanism, functionality, modeling and applications. *Prog Polym Sci* 2012;37: 1720–63.

- [2] Meng H, Li G. A review of stimuli-responsive shape memory polymer composites. *Polymer* 2013;54:2199–221.
- [3] Leng J, Lan X, Lu Y, Du S. Shape-memory polymers and their composites: stimulus methods and applications. *Prog Mater Sci* 2011;56:1077–135.
- [4] Gibson RF. A review of recent research on mechanics of multifunctional composite materials and structures. *Compos Struct* 2010;92:2793–810.
- [5] Behl M, Razzaq MY, Lendlein A. Multifunctional shape-memory polymers. *Adv Mater* 2010;22:3388–410.
- [6] Mather PT, Luo X, Rousseau IA. Shape memory polymer research. *Annu Rev Mater Sci* 2009;39:445–71.
- [7] Sun L, Huang WM, Ding Z, Zhao Y, Wang CC, Purnawali H, et al. Stimulus-responsive shape memory materials: a review. *Mater Des* 2012;33:577–640.
- [8] Santhosh Kumar KS, Biju R, Reghunadhan Nair CP. Progress in shape memory epoxy resins. *Reactive Funct Polym* 2013;73:421–30.
- [9] Liu Y, Han C, Tan H, Du X. Thermal, mechanical and shape memory properties of shape memory epoxy resin. *Mater Sci Eng A* 2010;527:2510–4.
- [10] Leonardi AB, Fasce LA, Zucchi IA, Hoppe CE, Soulé ER, Pérez CJ, et al. Shape memory epoxies based on networks with chemical and physical crosslinks. *Eur Polym J* 2011;47:362–9.
- [11] Rousseau IA, Xie T. Shape memory epoxy: composition, structure, properties and shape memory performances. *J Mater Chem* 2010;20:3431–41.
- [12] Feldkamp DM, Rousseau IA. Effect of chemical composition of the deformability of shape-memory epoxies. *Macromol Mater Eng* 2011;296:1128–41.
- [13] Xie T, Rousseau IA. Facile tailoring of thermal transition temperatures of epoxy shape memory polymers. *Polymer* 2009;50:1852–6.
- [14] Biju R, Reghunadhan Nair CP. Synthesis and characterization of shape memory epoxy-anhydride system. *J Polym Res* 2013;20:82.
- [15] Rousseau IA. Challenges of shape memory polymers: a review of the progress toward overcoming SMP's limitations. *Polym Eng Sci* 2008;48:2075–89.
- [16] Yakacki CM, Ortega AM, Frick CP, Lakhera N, Xiao R, Nguyen TD. Unique recovery behavior in amorphous shape-memory polymer networks. *Macromol Mater Eng* 2012;297:1160–6.
- [17] Feldkamp DM, Rousseau IA. Effect of the deformation temperature on the shape-memory behavior of epoxy networks. *Macromol Mater Eng* 2010;295:726–34.
- [18] Liu Y, Gall K, Dunn ML, McCluskey P. Thermomechanical recovery couplings of shape memory polymers in flexure. *Smart Mater Struct* 2003;12:947–54.
- [19] Pandini S, Bignotti F, Baldi F, Passera S. Network architecture and shape memory behavior of cold-worked epoxies. *J Intell Mater Syst Struct* 2013;24:1583–97.
- [20] Xie T, Xiao X, Cheng Y-T. Revealing triple-shape memory effect by polymer bilayers. *Macromol Rapid Commun* 2009;30:1823–7.
- [21] Wang Z, Song W, Ke L, Wang Y. Shape memory polymer composite structures with two-way shape memory effects. *Mater Lett* 2012;89:216–8.
- [22] Karger-Kocsis J, Friedrich K. Fatigue crack propagation and related failure in modified, anhydride-cured epoxy resins. *Colloid Polym Sci* 1992;270:549–62.
- [23] Kavitha Revathi A, Rao S, Srihari S, Dayananda GN. Characterization of shape memory behavior of CTBN-epoxy resin system. *J Polym Res* 2012;19:9894.
- [24] Revathi A, Rao S, Rao KV, Singh MM, Murugan MS, Srihari S, et al. Effects of strain on the thermomechanical behavior of epoxy based shape memory polymers. *J Polym Res* 2013;20:113.

838 CHAPTER 27 Recent advances in SMPs and composites

- AU:1
- [25] Liu Y, Sun H, Tan H, Du X. Modified shape memory epoxy resin composites by blending activity polyurethane. *J Appl Polym Sci* 2013;127:3152–8.
  - [26] Grishchuk S, Gryshchuk O, Weber M, Karger-Kocsis J. Structure and toughness of polyethersulfone (PESU)-modified anhydride-cured tetrafunctional epoxy resin: effect of PESU molecular mass. *J Appl Polym Sci* 2012;123:1193–200.
  - [27] Karger-Kocsis J, Kéki S. Shape memory biodegradable polyesters: concepts of (supra) molecular architecturing. *Express Polym Lett* 2014;8.
  - [28] Lützen H, Gesing TM, Kim BK, Hartwig A. Novel cationically polymerized epoxy/poly( $\epsilon$ -caprolactone) polymers showing a shape memory effect. *Polymer* 2012;53:6089–95.
  - [29] Luo X, Mather PT. Triple shape polymeric composites (TSPCs). *Adv Funct Mater* 2010;20:2649–56.
  - [30] Fejős M, Molnár K, Karger-Kocsis J. Epoxy/polycaprolactone systems with triple-shape memory effect: electrospun nanoweb with and without graphene versus co-continuous morphology. *Materials* 2013;6:4489–504.
  - [31] Yuan YC, Yin T, Rong MZ, Zhang MQ. Self healing in polymers and polymer composites. Concepts, realization and outlook: a review. *Express Polym Lett* 2008;2:238–50.
  - [32] Li Q, Zhang P. A self-healing particulate composite reinforced with strain hardened short shape memory polymer fibers. *Polymer* 2013;54:5075–86.
  - [33] Merline JD, Reghunadhan Nair CP, Gouri C, Sadhana R, Ninan KN. Poly(urethane-oxazolidine): synthesis, characterisation and shape memory properties. *Eur Polym J* 2007;43:3629–37.
  - [34] Biju R, Gouri C, Reghunadhan Nair CP. Shape memory polymers based on cyanate ester-epoxy-poly(tetramethyleneoxide) co-reacted system. *Eur Polym J* 2012;48:499–511.
  - [35] Huang WM, Yang B, Fu YQ, editors. *Polyurethane shape memory polymers*. Boca Raton, FL: CRC Press; 2012.
  - [36] Grishchuk S, Mbhele Z, Schmitt S, Karger-Kocsis J. Structure, thermal and fracture mechanical properties of benzoxazine-modified amine-cured DGEBA epoxy resins. *Express Polym Lett* 2011;5:273–82.
  - [37] Grishchuk S, Schmitt S, Vorster OC, Karger-Kocsis J. Structure and properties of amine-hardened epoxy/benzoxazine hybrids: effect of epoxy resin functionality. *J Appl Polym Sci* 2012;124:2824–37.
  - [38] Chow WS, Grishchuk S, Burkhart T, Karger-Kocsis J. Gelling and curing behaviors of benzoxazine/epoxy formulations containing 4,4'-thiodiphenol accelerator. *Thermochim Acta* 2012;543:172–7.
  - [39] Liu Y, Gall K, Dunn ML, McCluskey P. Thermomechanics of shape memory polymer nanocomposites. *Mech Mater* 2004;36:929–40.
  - [40] Hazelton CS, Arzberger SC, Lake MS, Munshi NA. RF actuation of a thermoset shape memory polymer with embedded magneto-electroelastic particles. *J Adv Mater* 2007;39(3):35–9.
  - [41] Iijima M, Kobayakawa M, Yamazaki M, Ohta Y, Kamiya H. Anionic surfactant with hydrophobic and hydrophilic chains for nanoparticle dispersion and shape memory polymer nanocomposites. *J Am Chem Soc* 2009;131:16342–16343.
  - [42] Liu Y, Han C, Tan H, Du X. Organic-montmorillonite modified shape memory epoxy composite. *Polym Adv Technol* 2011;22:2017–21.
  - [43] Beloshenko VA, Varyukhin VN, Voznyak YV. Electrical properties of carbon-containing epoxy compositions under shape memory effect realization. *Composites Part A* 2005;36:65–70.
  - [44] Lu H, Gou J, Leng J, Du S. Synergistic effect of carbon nanofiber and sub-micro filamentary nickel nanostrand on the shape memory polymer nanocomposite. *Smart Mater Struct* 2011;20:035017.



- [45] Ding J, Zhu Y, Fu Y. Preparation and properties of silanized vapor-grown carbon nanofibers/epoxy shape memory nanocomposites. *Polym Composites* 2014;35:412–7.
- [46] Xiong ZY, Wang ZD, Li ZF, Chang RN. Micromechanism of deformation in EMC laminates. *Mater Sci Eng A* 2008;496:323–8.
- [47] Wang ZD, Li ZF, Wang YS. Microbuckling solution of elastic memory laminates under bending. *J Intell Mater Syst Struct* 2009;20:1565–72.
- [48] Abrahamson ER, Lake MS, Munshi NA, Gall K. Shape memory mechanics of an elastic memory composite resin. *J Intell Mater Syst Struct* 2003;14:623–32.
- [49] Basit A, L'Hostis G, Durand B. High actuation properties of shape memory polymer composite actuator. *Smart Mater Struct* 2013;22:025023.
- [50] Basit A, L'Hostis G, Pac MJ, Durand B. Thermally activated composite with two-way and multi-shape memory effects. *Materials* 2013;6:4031–45.
- [51] Basit A, L'Hostis G, Durand B. Multi-shape memory effect in shape memory polymer composites. *Mater Lett* 2012;74:220–2.
- [52] Ivens J, Urbanus M, De Smet C. Shape recovery in a thermoset shape memory polymer and its fabric-reinforced composites. *Express Polym Lett* 2011;5:254–61.
- [53] Fejős M, Romhány G, Karger-Kocsis J. Shape memory characteristics of woven glass fibre fabric reinforced epoxy composite in flexure. *J Reinforced Plastics Composites* 2012;31:1532–7.
- [54] Fejős M, Karger-Kocsis J. Shape memory performance of asymmetrically reinforced epoxy/carbon fibre fabric composites in flexure. *Express Polym Lett* 2013;7:528–34.
- [55] Fejős M, Karger-Kocsis J, Grishchuk S. Effects of fibre content and textile structure on dynamic-mechanical and shape-memory properties of ELO/flax bicomposites. *J Reinforced Plastics Composites* 2013;32:1879–86.
- [56] Liu Y, Du H, Liu L, Leng J. Shape memory polymers and their composites in aerospace applications: a review. *Smart Mater Struct* 2014;23:023001.
- [57] Campbell D, Barrett R, Lake MS, Adams L, Abramson E, Scherbarth MR, et al. Development of a novel, passively deployed roll-out solar array IEEE aerospace conference proceedings. MT: Big Sky; 2006. p. 1–9.
- [58] Sofla AYN, Meguid SA, Tan KT, Yeo WK. Shape morphing of aircraft wing: status and challenges. *Mater Des* 2010;31:1284–92.
- [59] Kuder IK, Arrieta AF, Raither WE, Ermanni P. Variable stiffness material and structural concepts for morphing applications. *Prog Aerosp Sci* 2013;63:33–55.
- [60] Lake MS, Campbell D. The fundamentals of designing deployable structures with elastic memory composites IEEE aerospace conference proceedings. MT: Big Sky; 2004. p. 2745–56.
- [61] Tobushi H, Hayashi S, Hoshio K, Makino Y, Miwa N. Bending actuation characteristics of shape memory composite with SMA and SMP. *J Intell Mater Syst Struct* 2006;17:1075–81.
- [62] Ghosh P, Rao A, Srinivasa AR. Design of multi-state and smart-bias components using shape memory alloy and shape memory polymer composites. *Mater Des* 2013;44:164–71.
- [63] Ware T, Ellson G, Kwasnik A, Drewicz S, Gall K, Voit W. Tough shape-memory polymer-fiber composites. *J Reinforced Plastics Composites* 2011;30:371–80.
- [64] Wang R, Xiao X, Xie T. Viscoelastic behavior and force nature of thermo-reversible epoxy dry adhesives. *Macromol Rapid Commun* 2010;31:295–9.
- [65] Jarali CS, Raja S, Kiefer B. Modeling the effective properties and thermomechanical behavior of SMA-SMP multifunctional composite laminates. *Polym Composites* 2011;32:910–27.





## NON-PRINT ITEM

### Abstract

Preparation, properties, and applications of shape memory (SM) epoxy resin (SMEP)-based systems and composites have been surveyed in this chapter. SM polymers are capable of memorizing one or more temporary shapes and recovering to the permanent shape upon an external stimulus that is usually heat. The underlying mechanisms of SM actions are introduced and discussed. Emphasis was put to present the progress on SMEP and related composite systems and to discuss their potential for practical applications. Trends deduced for future developments include the combination of SM with additional functionalities, such as self-healing, sensing, actuation, and the creation of multifunctional smart material systems.

### Keywords

Shape memory polymer (SMP), shape memory alloy (SMA), shape fixity ratio, shape recovery ratio, recovery stress, shape programming, epoxy resin, multi-shape memory, thermoresponsive shape memory, composites, self-healing, interpenetrating network (IPN), conetwork, aerospace application, deployable structure



